Int. J. Electrochem. Sci., 7 **(2012)** 3543 - 3554

International Journal of
ELECTROCHEMICAL
SCIENCE
www.electrochemsci.org

Synthesis and Characterization of Novel Corrosion Inhibitor Derived from Oleic Acid: 2-Amino 5-Oleyl-1,3,4-Thiadiazol (AOT)

Sutiana Junaedi[1,*], *Abdul Amir H. Kadhum*[1], *Ahmed A. Al-Amiery*[1,2], *Abu Bakar Mohamad*[1], *Mohd Sobri Takriff* [1]

[1] Department of Chemical and Processing Engineering, Faculty of Engineering and Built Environment, National University of Malaysia, Bangi, Selangor 43600, Malaysia
[2] Biotechnology Division, Applied Science Department, University of Technology, Baghdad 10066, Iraq
[*]E-mail: sutianajnd10@gmail.com

Received: 23 January 2012 / *Accepted:* 3 March 2012 / *Published:* 1 April 2012

Novel corrosion inhibitor as a green chemical product namely derivative, 2-amino 5-oleyl-1,3,4-thiadiazol (AOT) was synthesized by cyclization of oleic acid. The new corrosion inhibitor was characterized by FT-IR and NMR spectroscopical methods. AOT was evaluated as corrosion inhibitor for mild steel in 1M of Hydrochloric acid solution using Potentiodynamic and Electrochemistry Impedance Spectroscopy (EIS) technique. Results obtained show that AOT acts as a good corrosion inhibitor for mild steel in HCl solution. Theoretical studies were also done for the novel compound AOT.

Keywords: Corrosion Inhibitor; Oleic acid phosphorousoxychloride; thiosemicarbazide; aminooleylthiadiazole.

1. INTRODUCTION

Mild steel is used as a structural material for vessels reactor, pipelines, tank etc. which are known to corrode invariably in contact with various solvents. From the view point of nation's economy and financial implications of corrosion hazard, it is necessary to adopt appropriate means and ways to reduce the losses due to corrosion and. In acidic/alkaline aqueous environments, its corrosion and prevention are well studied, however in non-aqueous solvents limited reports are available [1-4].

Thiadiazole compounds with wide applications in medicinal chemistry as antibacterial, antimicrobial, antidepressant, anti-inflammatory , antiviral, and human antifungal agents, and in agricultural science as potent fungicides, herbicides and insecticides [5-12]. Thiadiazole compounds have emerged as a new and potential class of corrosion inhibitors. The corrosion inhibiting behavior of thiadiazoles on mild steel in acidic media were reported by authors [13–16] A survey of the literature reveals that despite the high ability of thiadiazole compounds to strongly interact with metal surfaces, little attention has been made on the use of these compounds as corrosion inhibitors in hot acids.

The research area is primarily concerned to synthesize the corrosion inhibitor molecule by combination of natural products with synthetic chemical that environmentally friendly and ecologically acceptable. To predict the inhibition performance of the molecule target, the chemical structure evaluated by quantum theoretical method. The work is focused on the synthesis of amino oleyl thiadiazole which used oleic acid as raw material. Performance evaluation of the product and correlation between the molecular structure of the product and its inhibition efficiency, electrochemical studies such as potentiodynamic polarization and electrochemistry impedance spectroscopy were conducted.

2. THEORETICAL STUDY

2.1. Molecule Orbital

The electronic properties such as energy of the highest occupied molecular orbital (E_{HOMO}), energy of the lowest unoccupied molecular orbital (E_{LUMO}), energy gap (ΔE) between LUMO and HOMO and Mulliken charges on the backbone atoms were determined by optimization. The percent inhibition efficiencies increase if the molecules have higher HOMO energies and lower LUMO energies [17]. The percent inhibition efficiency increased with decrease in energy gap. The inhibitors can form coordination bonds between the unshared electron pair of the N atom and the unoccupied d electronic orbital of metal [18]. The larger the negative charge of N atom has, the better action is for the electronic donor.

2.2. Atomic charges

All chemical interactions are either electrostatic (polar) or orbital (covalent), electric charges in the molecule are obviously responsible for electrostatic interactions. The local electron densities or charges are important in many chemical reactions and for physico-chemical properties of compounds. Thus, charge-based parameters have been widely employed as chemical reactivity indices or as measures of weak intermolecular interactions. Despite its usefulness, the concept of a partial atomic charge is somewhat arbitrary, because it depends on the method used to delimit between one atom and the next. As a consequence, there are many methods to estimate the partial charges. Mulliken population analysis [18] is mostly used for the calculation of the charge distribution in a molecule. These numerical quantities are easy to obtain and they provide at least a qualitative considerate of the

structure and reactivity of molecules [19]. Furthermore, atomic charges are used for the description of the molecular polarity of molecules and Molecular orbital energies. Highest occupied molecular orbital energy (E_{HOMO}) and lowest unoccupied molecular orbital energy (E_{LUMO}) are very popular quantum chemical parameters. These orbitals, were also called the frontier orbitals, determine the way the molecule interacts with other species. The HOMO is the orbital that could act as an electron donor, since it is the outermost (highest energy) orbital containing electrons. The LUMO is the orbital that could act as the electron acceptor, since it is the innermost (lowest energy) orbital that has space to accept pairs of electrons.

Consistent with the frontier molecular orbital theory, the formation of a transition state is due to an interaction between the frontier orbitals (HOMO and LUMO) of reactants [20]. The energy of the HOMO is directly related to the ionization potential and the energy of the LUMO is directly related to the electron affinity. The HOMO–LUMO gap, i.e. the difference in energy between the HOMO and LUMO, is an important stability index [21]. A large HOMO–LUMO gap implies high stability for the molecule in chemical reactions [22]. The concept of ‘‘activation hardness” has been also defined on the basis of the HOMO–LUMO energy gap. The qualitative definition of hardness is closely related to the polarizability, since a decrease of the energy gap usually leads to easier polarization of the molecule [23].

3. EXPERIMENTAL

3.1. Synthesis and elucidation of 2-amino 5-oleyl-1,3,4-thiadiazol (AOT)

The inhibitor 2-amino 5-oleyl-1,3,4-thiadiazol (AOT) was synthesized by the cyclization reaction of oleic acid and thiosemicarbazide. Briefly, a mixture of phosphorylchloride (20 ml) was added to the oleic acid (0.05 mol) and the mixture was stirred for one hour at room temperature. Thiosemicarbazide (4.56 g, 0.05mol) was added and the mixture was heated under reflux for 24 hours. On cooling, the mixture was poured on to ice. After 4 hours, the mixture was stirred for 15 minutes, to decompose the excess phosphorusoxychloride, and then heated under reflux for 30 minutes; cool the mixture was neutralized by 5 % potassium hydroxide. The precipitated was filtered, washed with water, dried and re-crystallized from ethanol.

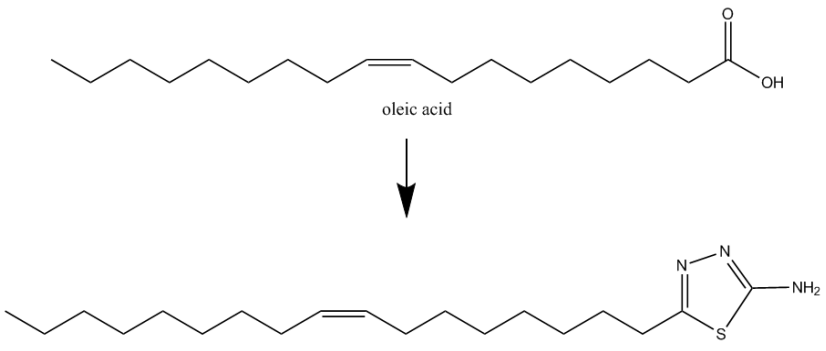

Figure 1. Amino Oleyl Thiadiazole (AOT) reaction formation

3.2. Inhibition Performance Test

Electrochemical measurements were conducted in a standard three-electrode cell. The counter electrode was a mesh of platinum of high purity (99.9%) and the reference electrode consisted of a saturated calomel electrode (SCE). The third electrode was the working electrode which was prepared from a round bar of carbon steel fixed in a cylindrical rod made out of Teflon. The cross-section area in contact with the solution was 1 cm^2. All of the tests were conducted in atmospheric at 30±1°C. Electrochemical testing was conducted using GAMRY galvanostat (Model 549) and digital multimeters (Fluke-73) through the galvanostatic polarization circuit.

The chemical composition of working electrode (wt) was C (0.21%), Si (0.36%), Mn (1.25%), P (0.025%), S (0.046%), Cr (0.16%), Ni (0.16%), Cu (0.41%), Mo (0.017%), Sn (0.017%), Al (0.003%), V (0.081%) and Fe (balance).

Before measurements, the surface of working electrode was mechanically abraded using different grades of abrasive papers, which ended with the 2000 grade. The disc was cleaned by washing with bidistilled water, thoroughly degreased with acetone, washed once more with bidistilled water and finally dried with a filter paper. For each test, a newly abraded electrode was used. The freshly polished electrode was pretreated further before each experiment by holding the potential at –1 V vs. a saturated calomel electrode for 1 min to reduce the oxide surface layer, and then open circuit potential (E-$_{ocp}$) was allowed to stabilize for 10 minutes.

The corrosion tests were conducted in 1.0 M HCl solution in the absence and presence of various AOT concentrations of which molecular structures are given in Fig. 1. HCl solutions (1.0 M) were prepared from concentrated HCl solution and diluted by distilled water. The concentrations of the inhibitors employed were varied from 10.0 to 50 ppm. All of the test solutions were prepared from analytical-grade chemical reagents in distilled water without further purification. For each experiment, a freshly prepared solution was used. The test solutions were opened to the atmosphere without stirring and the temperature was controlled thermostatically at 30^{o}C.

4. RESULTS AND DISCUSSION

4.1. Elucidation of 2-amino 5-oleyl-1,3,4-thiadiazol (AOT)

The synthesized compound of thiadiazol derivatives was established on the basis of FTIR and NMR spectral data in order to substantiate the structure of the compound. The synthesized compound of thiadiazol derivatives was established on the basis of FTIR and NMR spectral data in order to substantiate the structure of the compound. Based on the FTIR spectrum that the Compound showed absorption bands ranging from 670-715 cm^{-1} for C-S Hetero str. and 3460-3510 cm^{-1} for N-H str. 1575-1630 cm^{-1} for N-N str. 1430-1600 cm^{-1} for C-N Hetero str., 2840-3000 cm^{-1} for Aliphatic C-H str., 1575-1630 cm^{-1} for N-N str., but not showed any bands ranging 1700-1725 $cm^{-1}$for C=O str., 3500-3560 $cm^{-1}$for O-H str., and 1345-1400 $cm^{-1}$for C-O str., which ensures the absence of any acidic group in synthesized compounds.

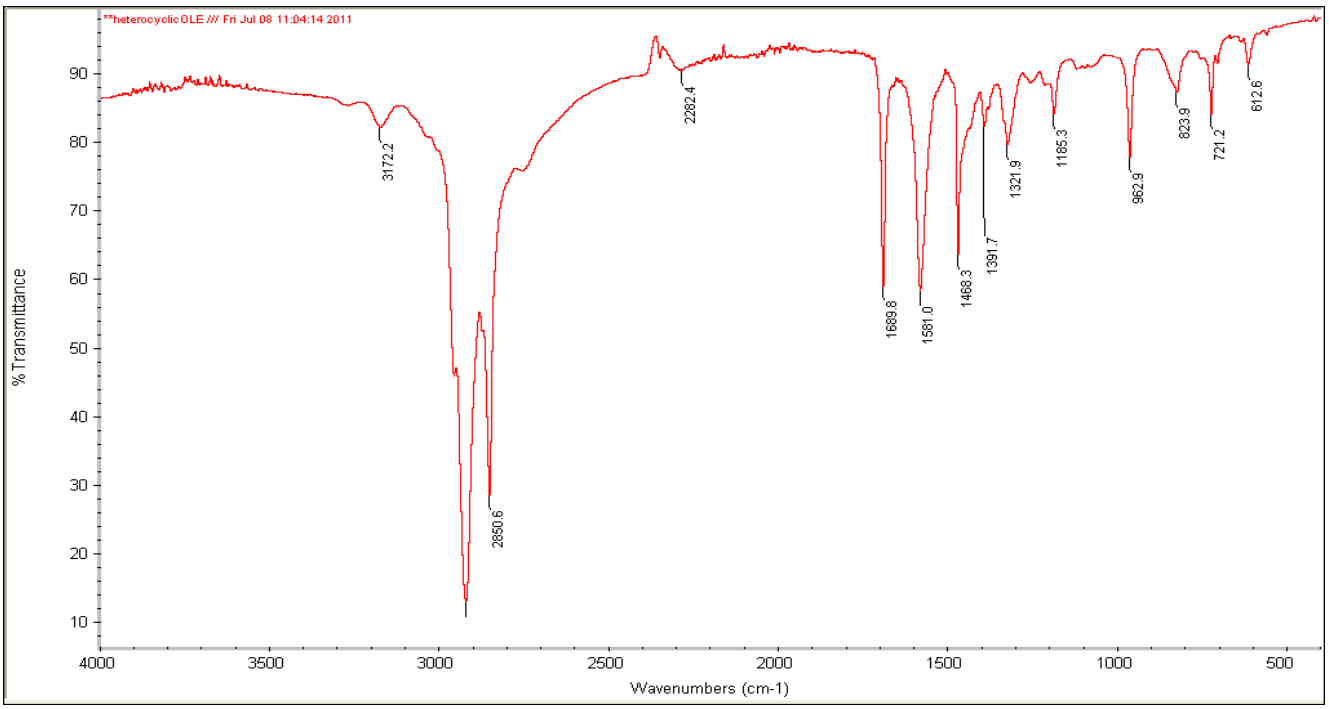

Figure 2. FTIR spectra of 2-amino 5-oleyl-1,3,4-thiadiazol *(AOT)*

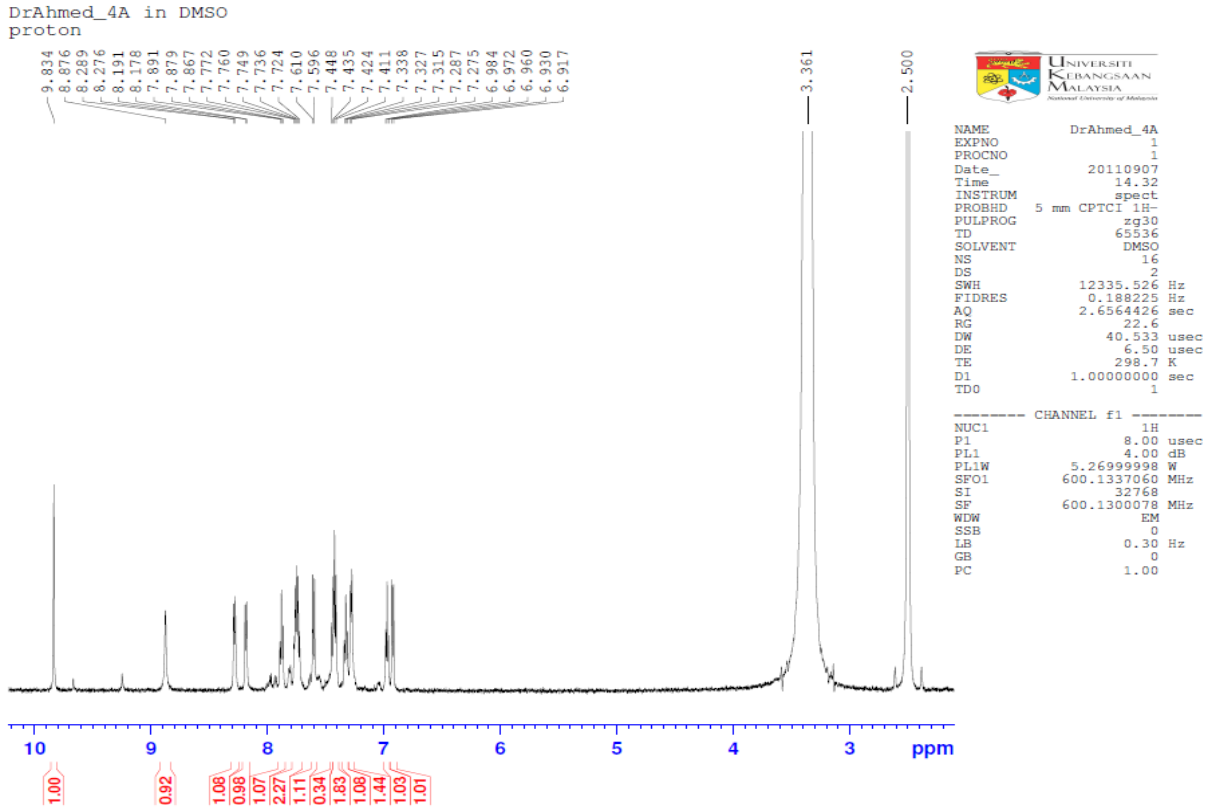

Figure 3. [1]HNMR spectrum of 2-amino 5-oleyl-1,3,4-thiadiazol *(AOT)*

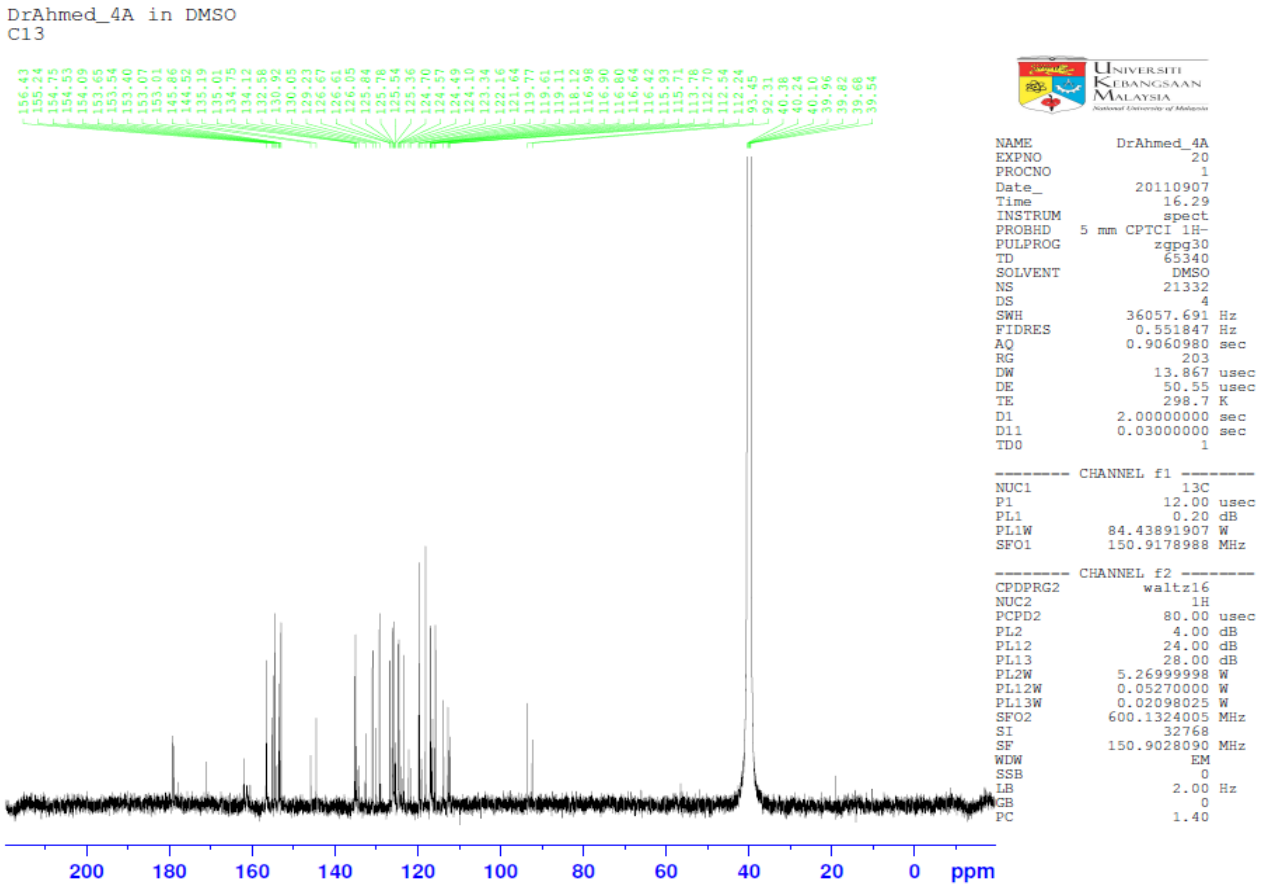

Figure 4. ^{13}CNMR spectrum of 2-amino 5-oleyl-1,3,4-thiadiazol *(AOT)*

Refers to NMR spectrum that the δ 3.957 ppm (N-H group of amine attached with thiadiazole), indicate the presence of above groups in the structure. The compound showed prominent singlet at δ 1.19-1.33, m, 4H and 1.34-1.81, m, 4H for subsequent protons of CH_3 groups present in aliphatic chain at the end of thiadiazole rings. The data above can be summarized ;yield 70%; 1H-NMR (CDCl3): δ 4.8 and 5.4 (dd, trans, H-C=C-H), δ 4.0 (s, NH_2), δ 1.20-2.0 (m, CH_2), δ 2.8 and 3.0 (tt, CH_2, C_2), δ 0.8 (t, CH_3); IR: 3172.2 cm-1 (NH_2, Amine), 2850 and 2930 cm-1 (CH, Aliphatic), 1689 cm^{-1} (C=C, Alkene), 1581 cm-1 (C=N, Imine). According to the FTIR, HNMR and ^{13}CNMR spectrum the data gives conformation of formation of thiadiazole ring, alkene, long chain alkane and amino group.

4.2. Potentiodynamic and Electrochemical Impedance Spectroscopy Measurement

The anodic and cathodic polarization curve recorded on mild steel in 1M of HCl at 30^{o}C in absence and presence of various concentration of AOT is shown in Fig 5. The cathodic current densities (I-corr) were determined by extrapolation of the cathodic Tafel lines to the corrosion potential (E-corr). In acid solution the anodic process of corrosion is the passage of metal ion from metal surface in to the solution and the principle cathodic process is the discharge of hydrogen ion to produce hydrogen gas or oxygen reduction.

The effect of the concentration of AOT was shown in Figure 5 which presents the anodic and cathodic Tafel curves of mild steel in 1 M of HCl. The inhibition efficiency (IE%) was calculated from polarization with AOT concentration for mild steel electrode in 1M of HCl solutions using equation 1 below:

$$IE\ (\%) = \left[\frac{io_{Corr.} - i_{Corr.}}{io_{Corr.}} \right] \times 100\% \qquad (1)$$

The result indicates that the I_{corr} decreased proportionally with increase inhibitor concentrations, that mean the metal dissolve in to the solution was decreased. The anodic and cathodic Tafel lines of mild steel in presence of AOT to be found was linear by increasing inhibitor concentrations. Values of anodic βa and cathodic βc Tafel constant and corrosion current density are listed in Table 1. This value was calculated from the intersection of the anodic and cathodic Tafel lines of the polarization curve at E_{corr}. The inhibition efficiencies are calculated without and with AOT in 1.0 M HCl solution.

Table1. Potentiodynamic polarization curves of mild steel in HCl 1M solutions at 30^{o}C in absence and presence of different concentration of AOT

Solutions	Parameters					
	βc, mVdec^{-1}	*E*-Corr, mV	βa, mVdec^{-1}	*i*Corr, _Acm^{-2}	CR, mpy	*IE(%)*
Blank	7.853	-613	1.988	1.250x10^{-3}	14.48	-
10ppm	123.2x10^{-3}	-607	99.1x10^{-3}	245.0x10^{-6}	2.841	80.4
20ppm	125.5x10^{-3}	-605	103.2x10^{-3}	217.0x10^{-6}	2.519	82.6
30ppm	134.3x10^{-3}	-603	121.7x10^{-3}	212.0x10^{-6}	2.456	83.0
50ppm	117.4x10^{-3}	-602	88.2x10^{-3}	136.0x10^{-6}	1.581	87.4

Fig. 6 shows a typical set of Nyquist plots for mild steel in 1M HCl in the absence and presence of AOT at various concentrations. It is apparent from these plots that the impedance response of mild steel in uninhibited HCl has significantly changed after the addition of AOT into the solutions. The impedance of inhibited mild steel increase with increase of AOT concentration, thus the efficiency is increases. R*ct* and C*dl* have opposite trend at the whole concentration range. It can be supposed that a protective layer covers the surface of the electrode. The inhibition efficiencies via EIS data were calculated through the following equation 2 below;

$$\%IE = \left[1 - \frac{R_{cto}}{R_{ct}} \right] x100 \qquad (2)$$

Where; R_{cto} and R_{ct} are the charge transfer resistance in the absence and presence of inhibitor, respectively. This plot is fitted to circuit model using Gamry Analyst software and the fitted value is listed in the table 2.

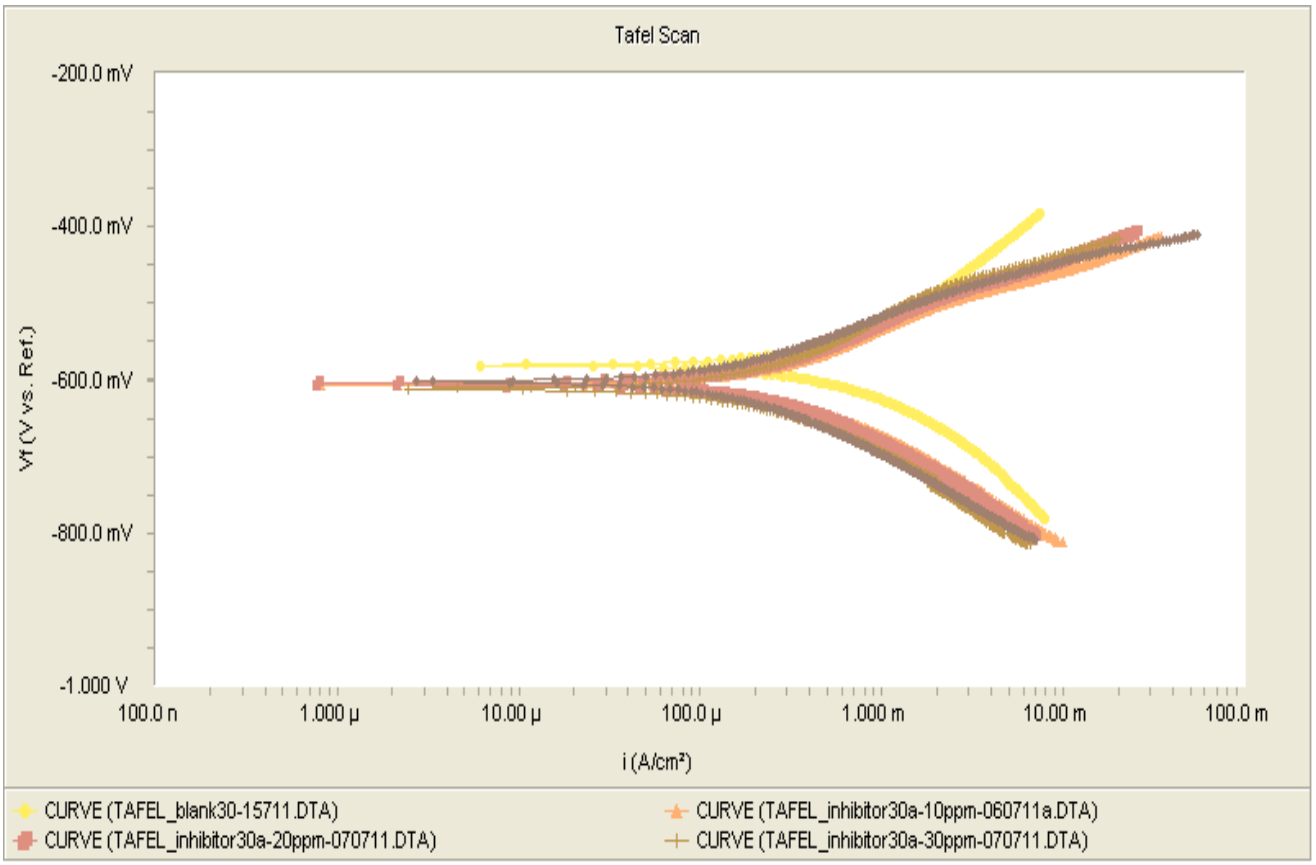

Figure 5. Potentiodynamic polarization curve of mild steel recorded in 1M HCl containing different concentration of AOT

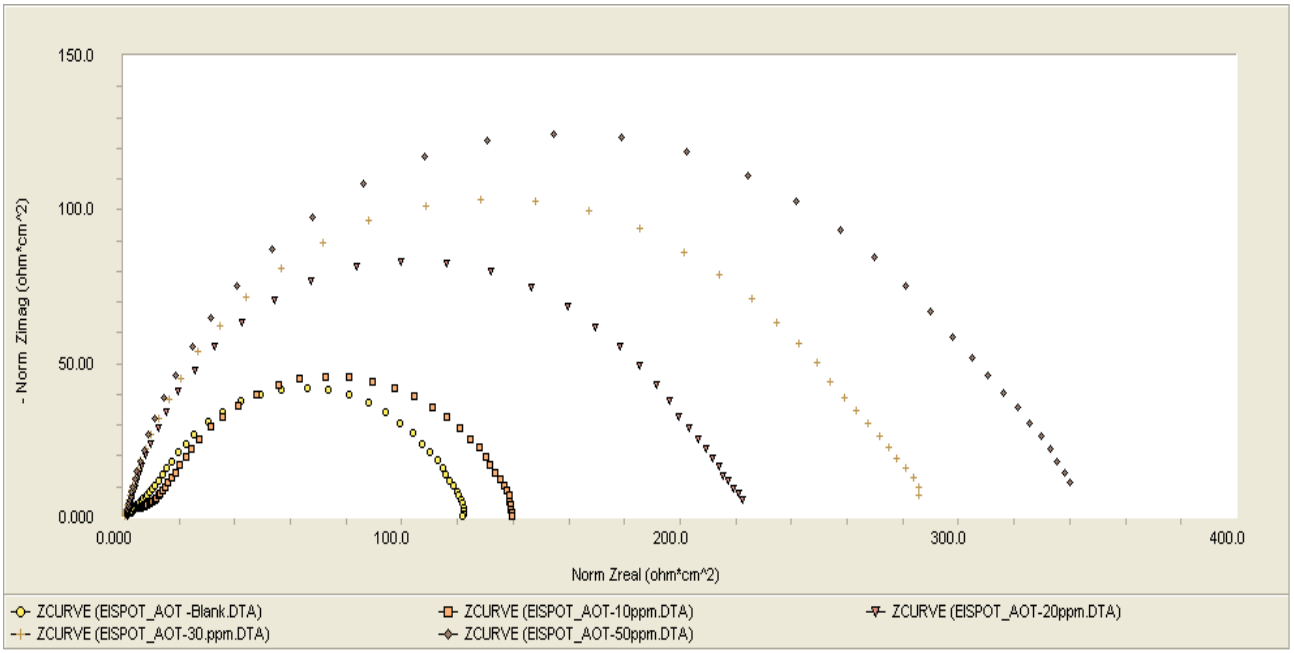

Figure 6. Nyquist plots for the mild steel in 1M HCl in the presence of mild steel recorded containing different concentration of AOT

Table 2. Fitted impedance parameter of mild steel in HCl 1M solutions at 30°C in absence and presence of AOT in different concentration

Solution	Parameter				
	Rct (Ohm cm^2)	Yo $u(Sxs^2cm^{-2})$	α	Cdl ($uFcm^2$)	IE %
Blank	29	$305x10^{-6}$	$446x10^{-3}$	$117x10^{-3}$	0
10ppm	110	$245x10^{-6}$	$623x10^{-3}$	$99x10^{-3}$	73
20ppm	125	$239x10^{-6}$	$655x10^{-3}$	$51x10^{-3}$	76
30ppm	157	$172x10^{-6}$	$846x10^{-3}$	$38x10^{-3}$	81
50ppm	188	$167x10^{-6}$	$865x10^{-3}$	$27x10^{-3}$	84

4.3. Quantum Chemical Calculation

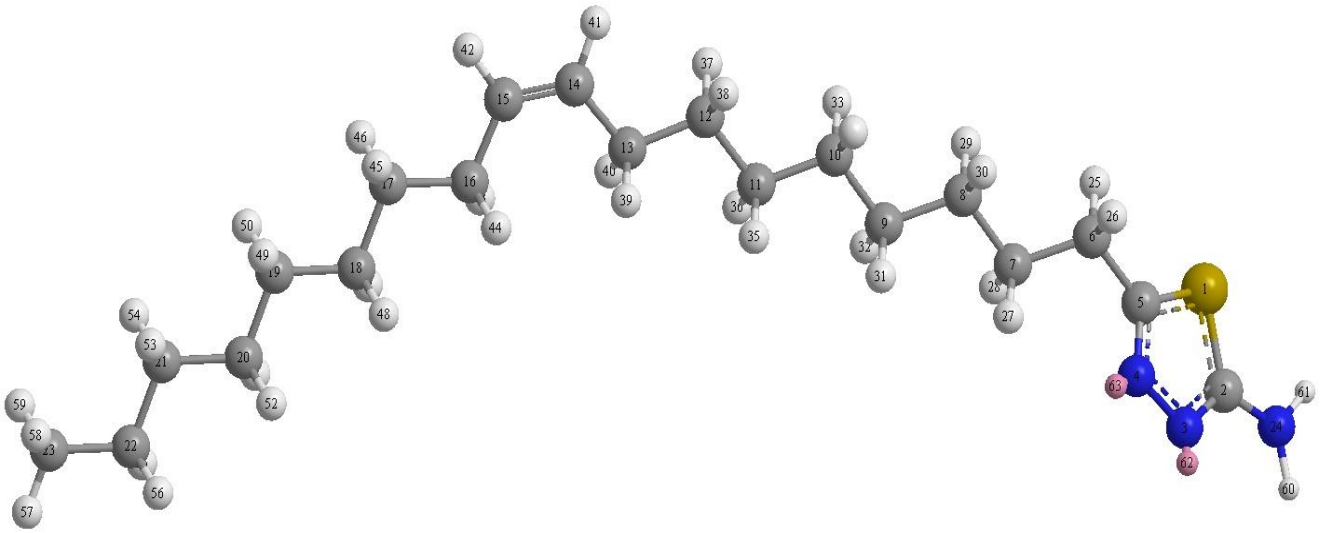

Figure 7. Chemical structure of 2-amino 5-oleyl-1,3,4-thiadiazol *(AOT)*

Inhibition of corrosion in acid solutions can be affected by the addition of a variety of organic molecules. Compounds containing nitrogen, oxygen and sulfur have shown vast applications as corrosion inhibitors.

The calculated orbital molecule density distribution of AOT was presented in Fig 7. The population of the HOMO concerned around the nitrogen and sulfur atoms in the AOT molecule. The value of E_{HOMO} and E_{LUMO} was calculated by using DFT listed in the table 3. The high inhibition efficiency of AOT can be attributed to the low value of ΔE.

The results of our present work show that AOT has good protective effect for mild steel and has small E_{HOMO} and E_{LUMO} values. Another point to be considered in energy level is the gap between the HOMO and LUMO energies for the inhibitors. The HOMO–LUMO gap for AOT is -8.923 eV obtained from E_{HOMO}-E_{LUMO} [(-)8.401 eV− (+)0.522 eV].

Table 3. Calculated Mulliken Atomic Charge of 2-Amino-5-Oleyl-1,3,4-Thiadiazole

Parameters					
Atomic No	Atom Type	Charge eV	Atomic No	Atom Type	Charge eV
1	S	+0.375	13	C	-0.059
2	C	+0.230	14	C	-0.052
3	N	-0.518	15	C	-0.052
4	N	-0.361	16	C	-0.059
5	C	+0.039	17	C	-0.050
6	C	-0.082	18	C	-0.057
7	C	-0.046	19	C	-0.055
8	C	-0.056	20	C	-0.055
9	C	-0.055	21	C	-0.054
10	C	-0.056	22	C	-0.047
11	C	-0.057	23	C	-0.129
12	C	-0.050	24	N	+0.052

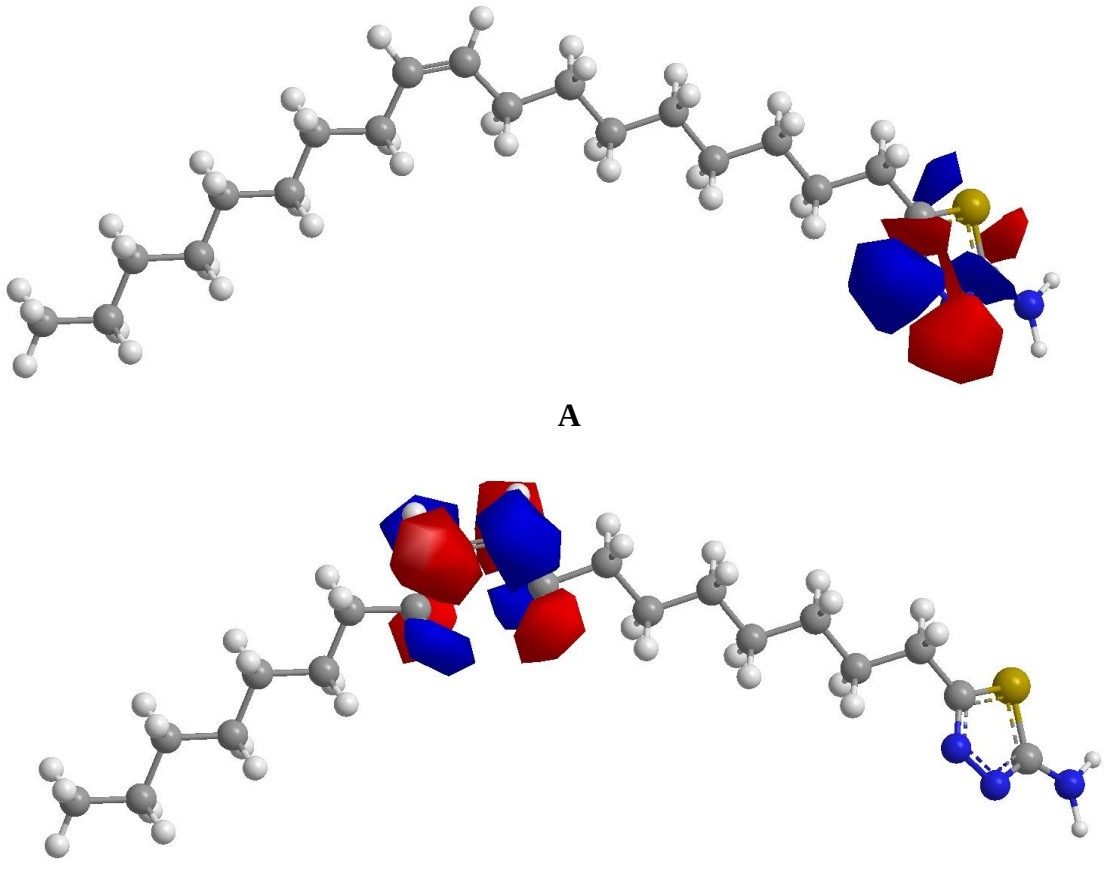

A

B

Figure 8. Molecular Orbital Plot of 2-amino 5-oleyl-1,3,4-thiadiazol *(AOT)* (*A*:HOMO *B*:LUMO)

The optimized molecular structures are given in Fig. 7 and the electronic properties in Table 3. The HOMO and LUMO energies are correlated with percent inhibition efficiencies. It has been reported that the higher the HOMO energy (E_{HOMO}) level of the inhibitor is, the greater is the ease of offering electrons to the unoccupied d orbital of metallic copper and the greater is the inhibition efficiency of the inhibitor [24].

As shown in Table 3, the positive charge density on one Nitrogen atoms in AOT molecule is small. The HOMO–LUMO energy gap was related to the redox potential. The small HOMO–LUMO energy gap implies soft–soft interaction will be expected [17].

It has been reported that the inhibitors can form coordination bonds between the unshared electron pair of the Nitrogen atom and the unoccupied *d* electronic orbital of metal [18]. Transition element has *d* orbital that can form coordination covalent bonding with nitrogen which has electron pairs act as *ligan*. Mulliken atomic charge values distribution of AOT as that all Nitrogen and Sulfur and small of Carbon atoms carry negative charges. This indicates that these atoms are negative charges center which can donate electron to the iron atom to form covalent coordinate bonding [15]. So, the effects of the presence of NH_2 group and Nitrogen atom in AOT have an ability to act as corrosion inhibitors as investigated by theoretical calculations.

This behavior was confirmed by potentiodynamic measurement where the changing in βa is more pronounced than βc. Table 3 also reveal that the electron charge density on Nitrogen atom no 3 as shown in the Figure 7 increase proportionally with inhibition ability of AOT. This indicates that Nitrogen atom no 3 is bonding center of the molecule or leads to the transfer of *chelation* center from each pair of nitrogen atom in inhibition studied. The larger negative charge of Nitrogen atom has, the better action is for the electronic donor. In general, AOT has the quiet strong interaction with steel and has the good inhibitory effect on atmospheric corrosion of steel in acid media.

5. CONCLUSION

2-amino 5-oleyl-1,-3,-4-thiadiazol (AOT) was synthesized and elucidated by FT-IR and NMR spectroscopy. The corrosion inhibition property was evaluated by potentiodynamic and electrochemical impedance spectroscopy methods. It has been proved that AOT has good protection effect. Molecule orbital theoretical calculations by the Density Functional Theory (DFT) method give the relationship between inhibition effect and the E_{LUMO}–E_{HOMO} values and the charge intensities of Nitrogen atoms. The active site of the molecule is located on Nitrogen atom in the heterocyclic ring (thia-diazole) and leads to the transfer of *chelation* center.

References

1. U. Ekpe, U. Ibok, B. Ita, O. Offiong and E. Ebenso, *Chem. Phy.*, 40 (1995**)** 87.
2. M. Onen, O. Maitera, J. Joseph and E. Ebenso, *Int. J. Electrochem. Sci.*, 6 (2011) 2884.
3. M. Quraisi and F. Ansari, *J. App. Electrochem.*, 36 (2006) 309.
4. M. Quraisi and F. Ansari, *J. App. Electrochem.*, 33 (2003) 233.

5. X. Weiming, S. Baoan, B. Pinaki, S. Yang and H. Deyu, *Molecules*, 15 (2010) 766.
6. E. Eno, A. David and O. Nnabuk, *Int. J. Mol. Sci.* 11 (2010) 2473.
7. S. Leokadia, *Int. J. Mol. Sci*. 7 (2006*)* 231.
8. M. Al-Smadi and F. Al-Momani, *Molecules* 13 (2008) 2740.
9. A. Kadhum, A. Al-Amiery, A. Musa and A. Mohamad, *Int. J. Mol. Sci.* 12 (2011) 5747.
10. A. Al-Amiery, A. Musa, A. Kadhum, and A. Mohamad, *Molecules*, 16 (2011) 6833. 10.3390/molecules16086833
11. A. Kadhum, A. Al-Amiery, M. Shikara and A. Mohamad, *Int. J. Phys. Sci.*, 6(2011) 6681.
12. A. Al-Amiery, Y. Al-Majedy, H. Abdulreazak and H. Abood, *Bioinorganic Chemistry and Applications*, 2011 (2011)1.
13. E. Azhar, B. Mernari, M. T raisnel, F. Bentiss and M. Legrenee, *Corr. Sci.*, 43 (2001**)** 2229.
14. M. Bentiss, M. Traisnel and M. Lagrenee, *J. App. Electrochem.*, 31 (2001) 41.
15. M. Lebrini, M. Lagrenee, H. Vezin, L. Gengembre and F. Bentiss, *Corr. Sci.*, 47 (2005**)** 485.
16. F. Bentiss, M. Lebrini, H. Vezin and M. Lagrenee, *Materials Chemistry Physics*, 87 (2004) 18.
17. V. S. Sastri and J. R Perumareddi, .*Corrosion*, 53 (1997**)** 617.
18. K. F. Khaled and M. A. Amin, *Corros. Sci.* 51 (2009**)** 1964.
19. A. Badiea and K. Mohana, *Corros. Sci.* 51 (2009**)** 2231.
20. Y. Tang, X. Yang, W. Yang, Y. Chen, R. Wan, *Corros. Sci.* 52 (2010**)** 242.
21. A.S. Fouda and A.S. Ellithy, *Corros. Sci.* 51 (2009**)** 868.
22. M. Ohsawa, W. Suetaka, *Corros. Sci.* 19 (1979**)** 709.
23. M.K. Pavithra, T. V . Venkatesha, K. Vathsala and K. O. Nayana, *Corros. Sci.* 52 (2010**)** 3811–3819.
24. J. Cruz, T. Pandiyan and E. Garcı´a-Ochoa, Journal of Electroanalytical Chemistry 583 (2005) 8.